

## Improved Corrosion Protection Properties in Anodic Films Type Porous on 2024 T3 Aluminium Alloys Obtained by Pulse Reverse Plating.

W. Aperador<sup>1,\*</sup>, A. Delgado<sup>1,2</sup>, J. Bautista<sup>3</sup>

<sup>1</sup>Departament of Engineering, Universidad Militar Nueva Granada, Carrera 11 No. 101-80, Fax:+57(1) 6343200, Bogotá, Colombia.

<sup>2</sup>Escuela Colombiana de Ingeniería – Julio Garavito, Bogotá, Colombia.

<sup>3</sup> Departamento de Física, Universidad Francisco de Paula Santander. Avenida Gran Colombia No 12E – 96. B Colsag. Edificio de Laboratorios. San José de Cúcuta. Norte de Santander. Colombia

\*E-mail: [g.ing.materiales@gmail.com](mailto:g.ing.materiales@gmail.com)

Received: 12 May 2013 / Accepted: 14 June 2013 / Published: 1 July 2013

---

This article presents the results of improvement in the electrochemical properties of porous type anodic films grown on aluminium alloy AA2024 T3, obtained with the techniques of direct current, pulsed direct current and reverse pulse current, through an electrolyte H<sub>2</sub>SO<sub>4</sub> al 15% v/v. Morphological analysis was used atomic force microscopy and scanning electron microscopy allowing to identify the films obtained with inverse pulse current have a grain size smaller than those obtained by the two other deposition techniques. The evaluation of corrosion resistance in the films, we used electrochemical impedance spectroscopy and anodic polarization curves Tafel. These evaluation techniques established that the reverse pulse current deposition can generate deposits which increase the corrosion resistance of the anodic film.

---

**Keywords:** pulse current, anodic films, atomic force microscopy, electrochemical impedance spectroscopy, Tafel.

### 1. INTRODUCTION

The aluminium alloys are widely used in the aeronautic industry, in which satisfy most requirements by its relation among weight and mechanical properties [1-3]. An important factor in that sector is the control of pitting corrosion phenomenon in marine environments. The pure aluminium has excellent corrosion resistance, but it decreases according to the alloying elements content. The heterogeneous microstructure of the alloys favors the corrosion. In particular, the used aluminium

alloys as structure components in aircraft, the 2024 and 7075 are susceptible to suffer pitting corrosion on the surface; in consequence, they present a high density of enabling surface defects propitious for the beginning of the cracks by fatigue. The produced pitting by intergranular corrosion can be reach different lengths depend on the environmental conditions and the exposition time [2, 4].

The aluminium has low mechanical resistance, whereby is used with other elements to form alloys, which improves its mechanical properties. Thereby, it is offered to the industry a wide variety of combinations with good mechanical and corrosion resistance [5, 8]. The best way of protect the material and its alloys against corrosive environments such as atmospheric and marines, is coat its surface with thick oxide layers. The industrial process used to achieve this protection is known as anodized, that consists in make grow an anodic film of  $Al_2O_3$  in a controlled manner at constant current or potential, over the aluminium and its alloys, acting as anodes in an electrochemical cell which contents a neutral or acid electrolyte. These anodized always use a low current density, whereby achieve the improvement of the mechanical properties; however, the corrosive properties do not improve front the base material. Therefore, it has proposed in several researches the current density variation [9, 11].

The electrocoating with pulsed current (PDC) and pulse reverse current (PRC) from the cyanide solutions [12, 14]. The application of pulsed current has allowed improving the quality of an important number of electrodeposition industrial processes. Through it, in comparison with the deposits obtained by the traditional technique of direct current (DC), is possible to obtain with the same or better quality, coatings of copper, nickel and zinc from sulfate solutions, and gold, copper and brass from cyanide solutions. [15, 17]

The aim of this work is to examine the electrochemical properties and perform the morphologic analysis of anodic films porous type obtained by DC, PDC and PRC techniques.

## 2. METHODOLOGY

As substrate was used laminae of aluminium alloy AA2024-T3 with an area of  $2\text{ cm}^2$ , prepared at mechanical polish. The specimens were cleaned by ultrasonic in a sequence of degreasing by alcohol immersion and pickling in sodium hydroxide at 5% of volume at  $60\text{ }^\circ\text{C}$  during 30 s, followed by wash with deionized water and immersed in nitric acid 50% volume to volume (v / v) at room temperature and time of 60s. Subsequently, they were flushed with deionized water and dried with hot air.

**Table 1.** Used parameters in the obtaining of the anodic films by DC, PDC and PRC techniques.

Technique	$J_{on}$ (mA/cm <sup>2</sup> )	$J_{off}$ (mA/cm <sup>2</sup> )	$t_{on}$ (ms)	$t_{off}$ (ms)
DC	20	-	-	-
PDC	1	8	2	100
	2	18	2	100
PRC	1	10	-2	100
	2	10	-4	100

As electrolyte was used a  $H_2SO_4$  solution at 15% volume to volume (v / v); the used time to obtain the coatings was 30 minutes at  $20^\circ C$  of temperature. The conditions for each test are described in the table 1.

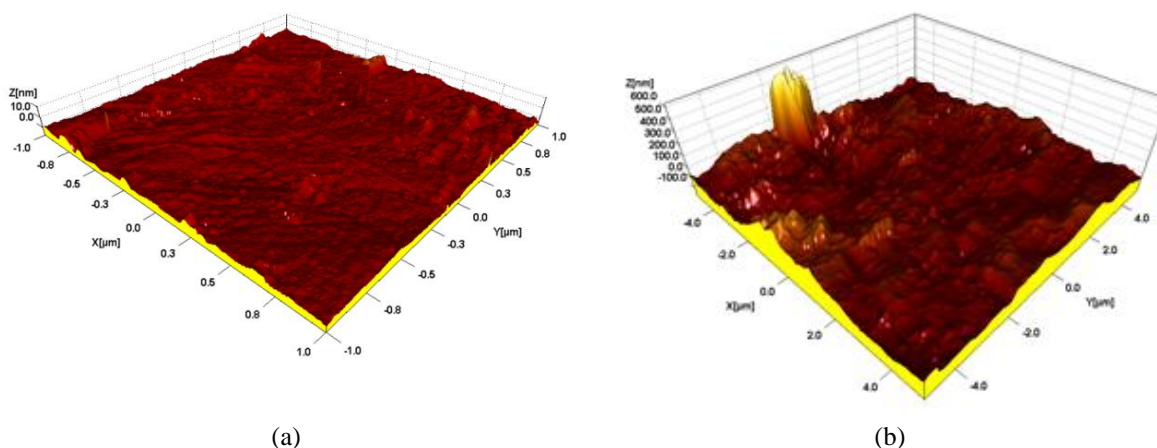
The characterization by scanning electron microscopy (SEM) was performed in the equipment Leo Electron Microscopy model 430. The grain size determination and the superficial analysis of the deposits were made using a scanning probe microscope in the mode of atomic force microscopy in contact (AFM). It was used a equipment MFP-3D™ of the Asylum Research. The rugosity measure was obtained with the *Scanning Probe Image Processor SPIP*® program in an area of  $1 \mu m^2$ . Furthermore, the fracture resistance was determinate by the Vickers microindentation technique, with a microdurometer HV 1000 series. For each specimen and in five different zones were performed 15 indentations with load of 2.94 N and time of 20 s.

In the electrochemical study was used a Gamry PCI 4 model equipment configured with EIS and Tafel techniques. These probes were developed at room temperature, using a cell composed by the working electrode, specimen for analyzing, with an exposition area of  $0.4 \text{ cm}^2$ , reference electrode of Ag/AgCl and graphite wire as auxiliary electrode in a solution of sodium chloride (NaCl) at 3.5% weight to volume (W/V). The working solution allows simulating marine conditions, in addition corrodes active metals forming chlorides on the metal. The Nyquist diagrams were obtained in a frequency range of 0.001 Hz to 100 kHz, amplitude of the sinusoidal signal of 10 mV and logarithmic frequency of 3 point by decade. The Tafel diagrams were obtained at a scanning velocity of 0.5 mV/s in a voltages range of -0.25 V to 0.45 V [18, 19].

### 3. RESULTS AND ANALYSIS

#### 3.1 Atomic Force Microscopy (AFM)

The superficial analysis of the aluminium substrate and the anodized are present in the figure 1. In the substrate topography (figure 1a) is observed a uniform surface, with minimum rugosity, as a result of the polishing treatment.



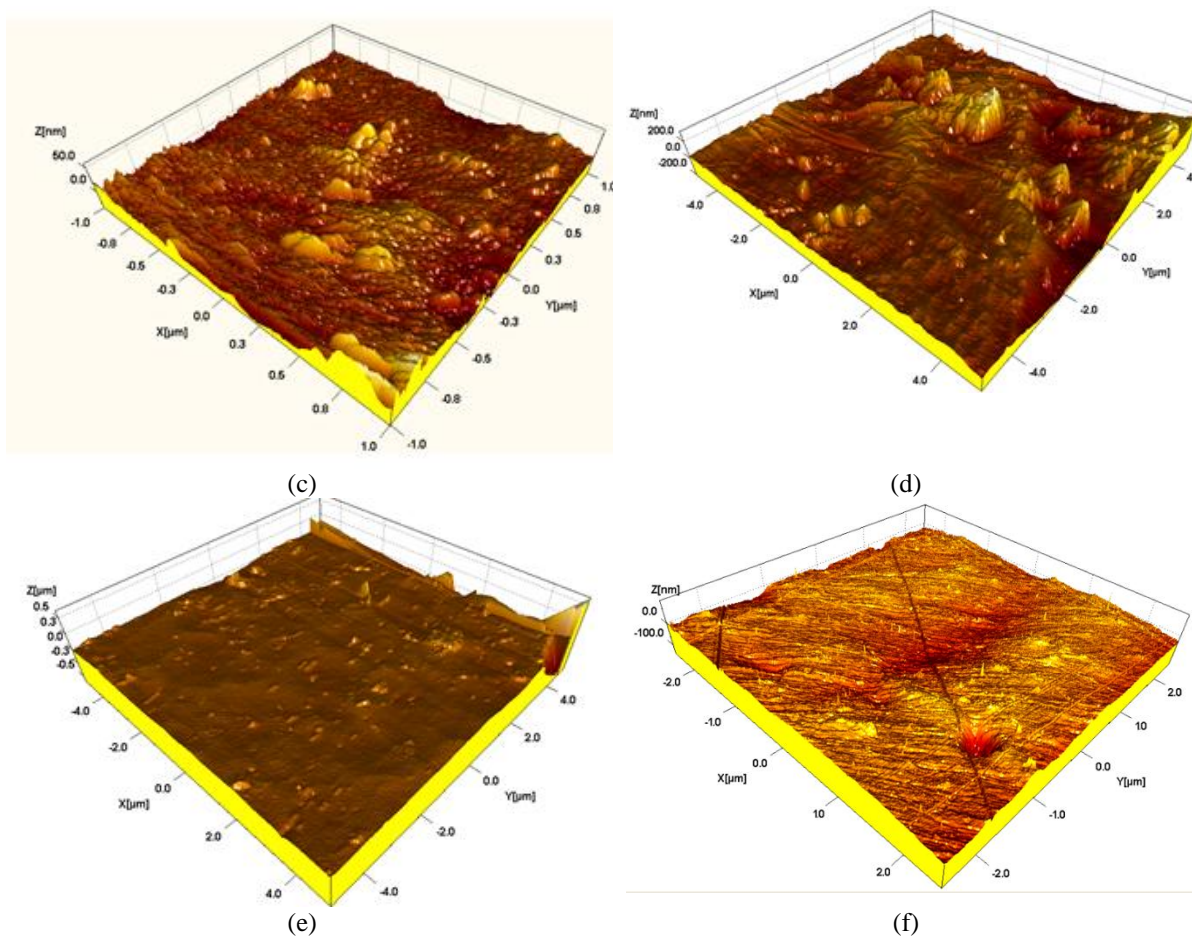


**Figure 1.** Topography obtained by AFM of the substrate and anodic films treated with the different techniques.

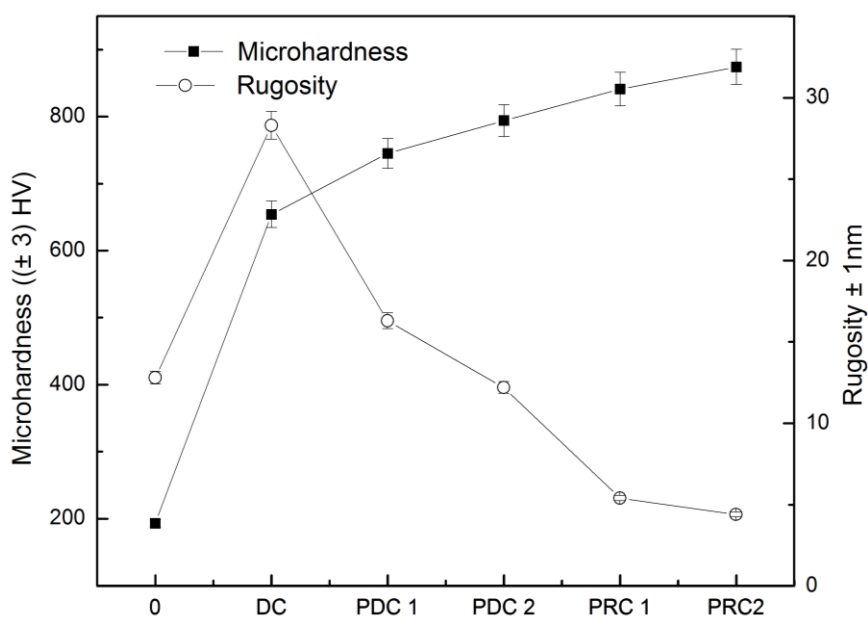


**Figure 2.** Relation among the values of rugosity and microhardness in function of the coatings by the DC, PDC and PRC techniques.

The figure 1b correspond to the anodized at  $\text{mA}/\text{cm}^2$ ; the rugosity and the heterogeneity of the surface have increased due to the superficial change process reach with the current density. The figures 1c and 1d illustrate the coating obtained by PDC technique; is observed the topology of the anodized very heterogeneous and quite irregular with rugosity values of 18 nm for PDC 1 and 13 nm for PCD 2. This indicates that increasing the current density ( $18 \text{ mA}/\text{cm}^2$ ) the rugosity of the obtained coating decrease.

The figures 1e and 1f show the details of the coatings obtained by the PRC technique. In contrast with the films deposited by DC and PDC techniques, is observed in the two images greater uniformity and homogeneity, which generates a superficial texture more fine.

The figure 2 related the rugosity values in function of the films obtained by the DC, PDC and PRC techniques. This figure confirms the mentioned situations above.

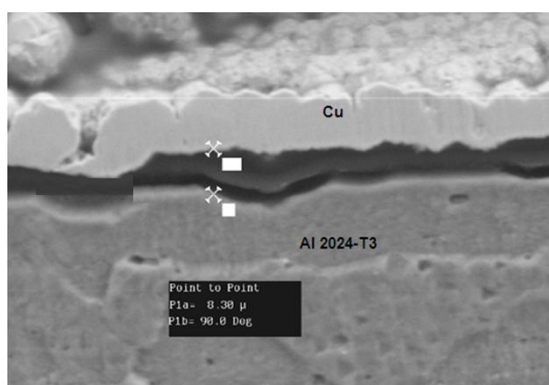
### 3.2 Vickers microhardness

The graph of the figure 2 shows the Vickers microhardness values for the substrate and the obtained films applying the conformed techniques. In the mentioned figure, the Vickers microhardness of the substrate is the 197 HV, inferior value in comparison with the values of each one of the studied anodic films [20]. The thicknesses of the anodized are small (measured with SEM). The specimens obtained by PRC technique offer the highest microhardness value among the others techniques.

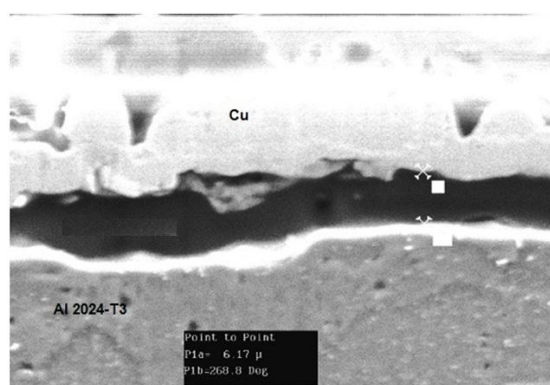
By correlating the values of the microhardness with the rugosity for the anodized, it is observed increase in the microhardness when the rugosity decreases. This effect is more representative in the films obtained by the pulsating techniques direct and reverses, due to the formation of an oxide film more compact, uniform and adherent on the aluminium substrate [21].

### 3.3 Scanning electron microscopy

To determinate the thickness of the films was proceeded to cut transversely. Due to the fragility of the films, was applied a cooper coating and was measured with the reference microscopy MEB LEO 430.



(a)



(b)

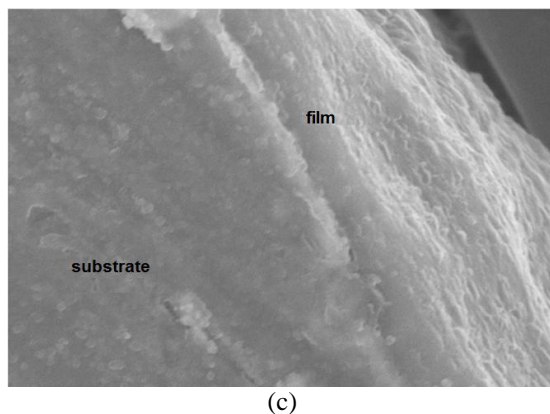


**Figure 3.** SEM micrographs at 5000X of the films grown by the techniques: (a) DC, (b) PDC1 and (c) PRC1.

The found results, according to the thickness of the films obtained by the deposition techniques, were:  $(9.11 \pm 0.2) \mu\text{m}$  by DC;  $(10.22 \pm 0.2) \mu\text{m}$  for the PDC1,  $(10.58 \pm 0.2) \mu\text{m}$  for the PDC2;  $(11.22 \pm 0.2) \mu\text{m}$  for the PRC1 y  $(11.54 \pm 0.2) \mu\text{m}$  for the PRC2 type. The thickness of the fine layer of aluminium oxide naturally present is  $(2.5 \pm 0.2) \mu\text{m}$ . In the case of the obtained oxide layers is presented thicknesses between 9 and  $12 \mu\text{m}$ . Importantly, that the above information corresponds to the average of ten measurements for each anodized film [23].

### 3.4 Electrochemical behavior

The anodic polarization curves are visualized in the figure 4. It is observed the presence of initial corrosion of the substrate, AA2024 T3 alloy. This type of alloy is mainly aluminium mixed with a copper percentage, which exists in solid solution translated in an alteration in the cathodic potential. The substrate presents a behavior change in the anodic branch at potential of  $-610 \text{ mV}$  vs. Ag/AgCl approximately. This change can be distinguish as the beginning of the formation of a slight passivating layer, with weak stability, since reaching this potential is observed the gradual increasing of the current density. Accompanied this phenomenon, is found the plateau in a range of  $-600$  to  $-900 \text{ mV}$  vs. Ag/AgCl, which can be indicate the regeneration of a corrosion product layer that allow to stabilize the current density around this potential range and avoid the increasing of the dissolution velocity of the anodized [23][24].

For the anodic films obtained by the DC, PDC and PRC techniques, it is observed general dissolution in the anodic region, which is superior for the coatings by the DC technique. Due to its greater value of corrosion current density, these dissolutions are dominated by the diffusion. For the films grown by PDC and PRC, are found positive values. The current values for these films are lower that the obtained with the DC technique and the substrate, which allow ensure that PRC technique give very good conditions for films growing, with a lower pore size, that improves the behavior of the alloy against aggressive mediums. The optimal anticorrosive behaviors were obtained with PRC 2. In the table 2 is presented the values of the parameters in each studied conditions.

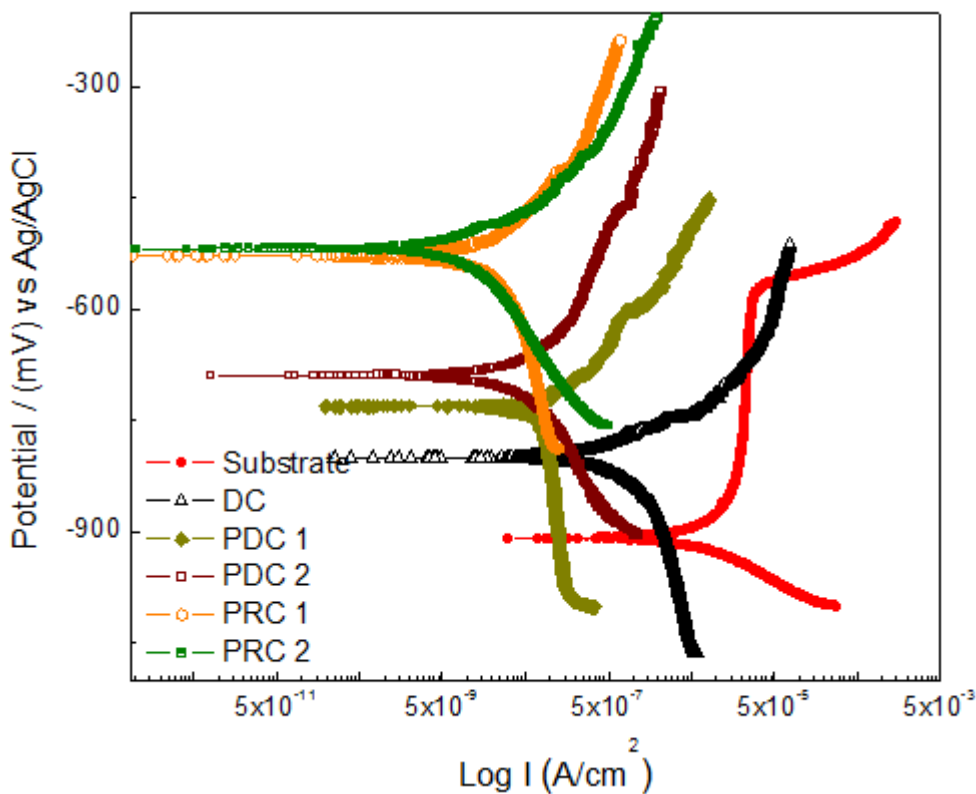


**Figure 4.** Tafel polarization curves for AA2024 T3 and anodic films growing by the DC, PDC and PRC techniques.

In the table 2 is shown the calculated parameters from the anodic polarization curves, which were found with the help of the Stern–Geary equation to calculate corrosion current densities that change in function of the used technique for the obtaining of the anodic films. Corrosion potentials more cathodic are observed for the DC, PDC and PRC techniques than the substrate; the obtained films with the pulsing techniques indicate corrosion potential close among them and this is owing to the obtaining parameters. The using of the pulsing techniques increases the relation of cathodic/anodic areas in the anodized matrix [16, 18], therefore the corrosion density and velocity decrease with the using of PDC and PRC techniques.

**Table 2.** Parameters obtained by the polarization curves for the Dc, PDC and PRC techniques.

Technique	$\beta_a$ (V/decade)	$\beta_c$ (V/decade)	$I_{corr}$ (A/cm <sup>2</sup> )	$E_{corr}$ (mV)	$V_{corr}$ (μmy)
Substrate	$163.7 \cdot 10^{-3}$	$272.1 \cdot 10^{-3}$	$1.3 \cdot 10^{-5}$	-906	304
DC	$120.6 \cdot 10^{-3}$	$1.870 \cdot 10^{-3}$	$1.6 \cdot 10^{-6}$	-801	37.3
PDC1	$94.80 \cdot 10^{-3}$	$146.0 \cdot 10^{-3}$	$1.48 \cdot 10^{-7}$	-731	3.45
PDC2	$260.3 \cdot 10^{-3}$	$366.6 \cdot 10^{-3}$	$7.53 \cdot 10^{-8}$	-688	1.75
PRC1	$64.30 \cdot 10^{-3}$	$94.9 \cdot 10^{-3}$	$3.34 \cdot 10^{-8}$	-527	0.78
PRC2	$75.6 \cdot 10^{-3}$	$111.2 \cdot 10^{-3}$	$1.34 \cdot 10^{-8}$	-519	0.313

The electrochemical impedance spectroscopy was applied with the purpose to evaluate and discriminate the process that occur during the electrochemical test over the AA2024 T3 alloy and the anodized when are in contact with the sodium chloride (NaCl) solution.

For the AA2024 T3 specimens are obtained a small semicircle in comparison with the anodized, which indicates a lower resistance value for the AA2024 T3 (figure 5).

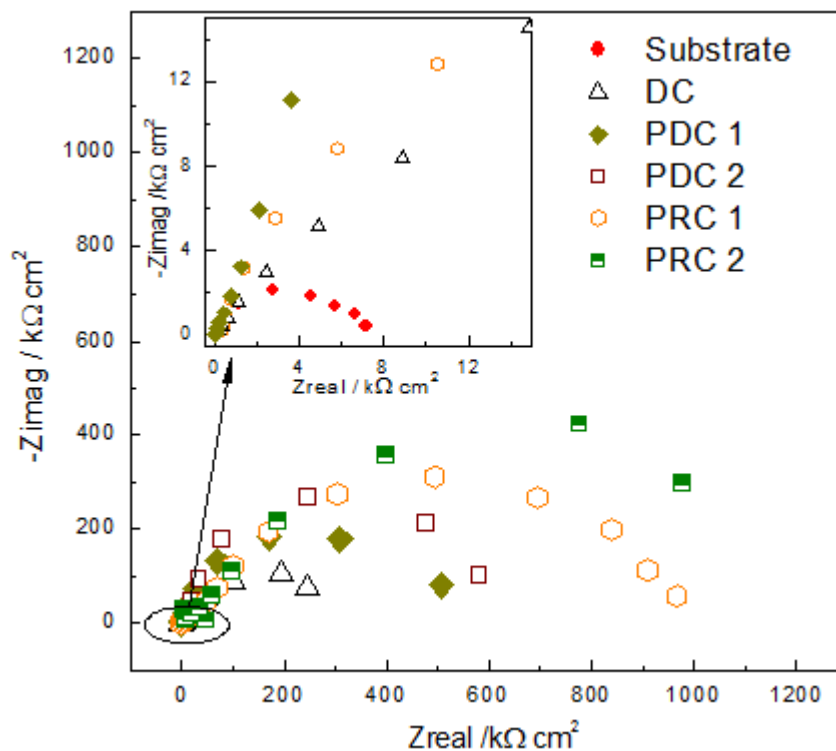


**Figure 5.** Nyquist diagram of the AA 2024 T3 substrate and the anodic films.

In the figure 6 is presented the equivalent electric circuit for the substrate case. This circuit is composed by a constant phase element connected in parallel with the charge transfer resistance, and in series with the solution resistance.

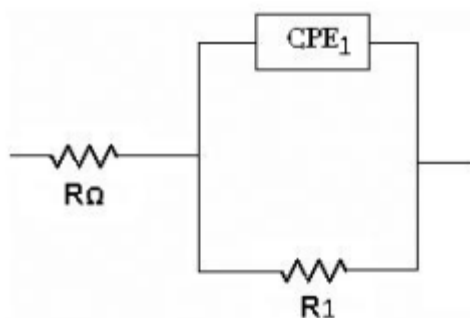


**Figure 6.** Equivalent circuit used to adjust the data of substrate impedance.

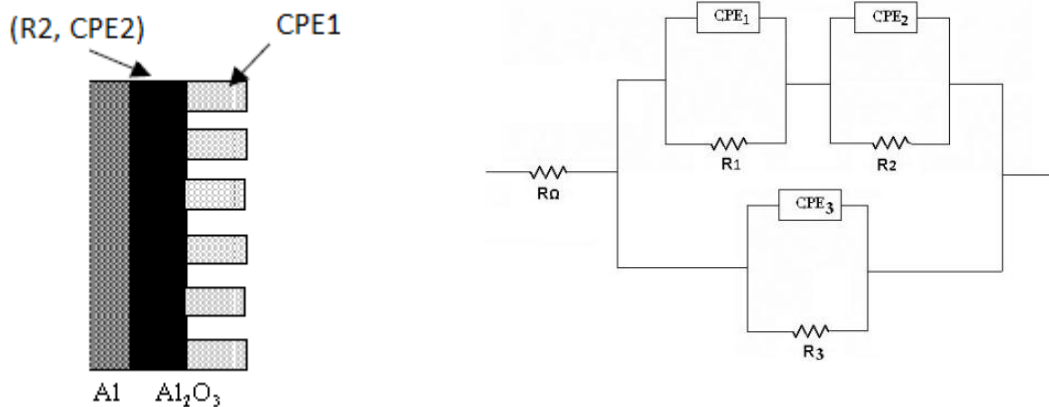


**Figure 7.** Equivalent circuit used to adjust the data of impedance of the anodic films obtained by the DC, PDC and PRC techniques.

**Table 3.** Used parameters for the adjustment of the impedance data of the substrate and anodic films.

	$R_{\Omega}$	$CPE_1$	$a_1$	$R_1$	$CPE_2$	$a_2$	$R_2$	$CPE_2$	$a_2$	$R_2$
	$\Omega \text{ cm}^2$	$\text{mF cm}^{-2} \text{ s}^{-(1-\alpha_1)}$		$10^3 \Omega \text{ cm}^2$	$\text{mF cm}^{-2} \text{ s}^{-(1-\alpha_2)}$		$10^3 \Omega \text{ cm}^2$	$\text{mF cm}^{-2} \text{ s}^{-(1-\alpha_2)}$		$10^3 \Omega \text{ cm}^2$
PRC2	51.11	44.21	0.86	8.42	185.5	0.84	580.3	254.34	0.84	974.7(8%)
	-	-4%	(0.5%)	-4%	-4%	-	-5%	-4%	-	
	0.50%					0.70%			0.50%	
PRC1	43.12	37.21	0.75	12.2	64.21	0.94	159.46	153.21	0.94	859.32 (4%)
	-	-4%	-	-5%	-2%	-	-6%	-2%	-	
	0.40%		0.40%			0.60%			0.60%	
PDC2	52.5	84.14	0.82	9.11	54.11	0.78	84.21	97.44	0.75	628.21(3%)
	-	-7%	-	-5%	-3%	-	-5%	-4%	-	
	0.50%		0.50%			0.30%			0.40%	
PDC1	64.8	36.43	0.87	11.21	51.24	0.76	92.91	80.24	0.79	592.91 (4%)
	-	-4%	-	-3%	-4%	-	-4%	-3%	-	
	0.50%		0.60%			0.50%			0.50%	
DC	51.5	29.98	0.84	9.17	21.54	0.66	84.98	65.54	0.75	248 (3%)
	-	-5%	-	-6%	-5%	-	-3%	-6%	-	
	0.40%		0.90%			0.70%			0.70%	
Substrate	53.1	11,28	0.74	8.07						
	-	-5%	-	-5%						
	0.60%		0.50%							

In the figure 7, for the anodic films obtained by the DC, PDC and PRC techniques, is observed various semicircles. This implies the conformation of three constant phase elements ( $CPE_1$ ,  $CPE_2$  y  $CPE_3$ ), representing in the diagram of the figure 7, where the elements  $CPE_1$ - $R_1$  are presented at high frequencies and are associated with reactions occurring around the passivating surface oxide layer. A second set of elements  $CPE_2$ - $R_2$ , are presented at intermediate frequencies, these are related with the barrier layer generated by the thickness of the anodized. Finally, a third set of elements  $CPE_3$ - $R_3$ ,

found at very low frequencies (1 mHz), is due to the charge transference and represents the response to the process that occurs in the system, which are slow in the obtained anodized.

For all the films grown by the DC, PDC and PPC techniques are obtained: the existence of superficial oxide layers together with the layer that serves of barrier, represented by the  $CPE_1-R_1$  y  $CPE_2-R_2$  elements, whose values are registered in the table 3. Regarding this, is inferred the existence of denser films than those obtained by the PDC and PRC techniques due to the highest values of the parameters, which represents the interface between the anodic film and the aluminium AA 2024 T3 substrate. The layer related with the set of elements  $CPE_3-R_3$  represents the charge transference. For the films obtained by the three deposition techniques, the resistance values to the polarization change. The more representative are of the pulsing techniques.

#### 4. CONCLUSIONS

- The anodic films of porous type obtained on the aluminium alloy AA 2024 T3, present greater homogeneity, mechanical resistance and lower dislocations density, when they are obtained by pulsing techniques, in special with the reverse pulse technique.
- The electrochemical behavior of the anodic films of porous type grown on the AA 2024 T3 and obtained with the pulsed current technique, show increase in the polarization resistance and capacitance of the double layer, in comparison with the traditional technique DC. Likewise, it was presented decrease in the potential values and corrosion current which indicates a lower corrosion velocity, improving the behavior of the anodic films obtained by pulsing techniques against aggressive mediums.
- The increase of the parameter cathodic and anodic voltage in the PDC and PRC techniques respectively, generated a better behavior in the mechanical and electrochemical properties; these behaviors were optimized due to the obtained lowest rugosity value owing to the coatings homogeneity.

#### ACKNOWLEDGEMENTS

The authors of the work express their gratitude to the Universidad Militar Nueva Granada.

#### References

1. G. Mable Pinto, J. Nayak, A. Nityananda Shetty, *Int. J. Electrochem. Sci.*, 4 (2009) 1452
2. W. Aperador, J. Caballero-Gómez, A. Delgado, *Int. J. Electrochem. Sci.*, 8 (2013) 6154
3. M. Bethencourt, F.J. Botana, M.J. Cano, M. Marcos, J.M. Sánchez Amaya, L. González Rovira, *Corrosion Science*, 51 (2009) 518
4. S. Valizadeh, E.B Svedberg, P. Leisner, *Journal of Applied Electrochemistry*, 27 (2002) 97

5. H. Ashassi-Sorkhabi, A. Hagrah, N. Parvini-Ahmadi, J. Manzoori, *Surface and Coatings Technology*, 140 (2001) 278
6. H. Chi-Chang, W. Chi-Ming, *Surface and Coatings Technology*, 176 (2003) 75
7. A. Stankeviciute, K. Ieinas, G. Bikulcius, D. Virbalyte, *Journal of applied electrochemistry*, 28 (1998) 89
8. J. Aldykewicz, H.S. Isaac, A.J. Davenport. *J. Electrochem. Soc.* 142 (1995) 3342
9. W. Bensalah, K. Elleuch, M. Feki, M. Wery, M.P. Gigandet, H.F. Ayedi. *Mater. Chem. Phys.* 108 (2008) 296
10. J.P. Sullivan, G.C. Wood, *Proc. Roy. Soc. Lond.* 317 (1970) 511–543.
11. S.W. Dean, W.H. Anthony. *Degradation of metals in atmosphere*. American society of testing and materials, Philadelphia (1988)
12. H.M. Obispo, L.E. Murr, M. Arrowood, E.A. Trillo, *J. Mater. Sci.* 35 (2000) 3479
13. J.V. Kloet, A.W. Hassel, M. Stratmann, *Z. Phys. Chem.* 219 (2005) 1505
14. L. Lacroix, L. Ressler, C. Blanc, G. Mankowski. *J. Electrochem. Soc.* 155 (2008) 131
15. T.J. Warner, M.P. Schmidt, F. Sommer, D. Bellot. *Z. Metallkd.* 86 (1995) 494
16. P. Campestrini, E.P.M. Van Westing, H.W. Van Rooijen, J.H.W. De Wit. *Corros. Sci.* 42 (2000) 1853
17. J.W. Silva, A.G. Bustamante, E.N. Codaro, R.Z. Nakazato, L.R.O. Hein. *Appl. Surf. Sci.* 236 (2004) 356
18. G.O. Llevbare. *Corrosion.* 56 (2000) 227
19. W. Aperador, E. Vera, L. M. Ipaz., *Revista EIA*, 15 (2011) 9.
20. S. jiang, P. Luo, H.H. Zhou, C. P Fu, Y.F. Kuang, *Transactions of Nonferrous Metals Society of China*, 18(2008)825.
21. H. Shih, S. Tzou, *Surface and Coatings Technology*, 124 (2000)278.
22. B. Fori, P. Taberna, L. Arurault, J. Bonino, C. Gazeau, P. Bares, *Colloids and Surfaces A: Physicochemical and Engineering Aspects*, 415(2012)187.
23. Y. Ma, X. Zhou, G.E. Thompson, M. Curioni, X. Zhong, E. Koroleva, P. Skeldon, P. Thomson, M. Fowles, *Corrosion Science*, 53 (2011) 4141.
24. S. A. Fadhil, Q. Mohsen, *Applied Surface Science*, 256 (2010) 5849.